Multiple homoclinic bifurcations from orbit-flip

I: Successive homoclinic doublings

Dedicated to Prof. L. P. Shil'nikov for his sixtieth birthday

Hiroshi Kokubu*
Department of Mathematics, Kyoto University
Kyoto 606-01, Japan
kokubu@kusm.kyoto-u.ac.jp

Motomasa Komuro
Department of Mathematics
The Nishi-Tokyo University
Yamanashi 409-01, Japan

and

Hiroe Oka†
Department of Applied Mathematics and Informatics
Faculty of Science and Technology
Ryukoku University
Seta, Otsu 520-21, Japan
oka@rins.ryukoku.ac.jp

*Research was supported in part by Grant-in-Aid for Scientific Research (No. 06740150, 07740150), Ministry of Education, Science and Culture, Japan.

†Research was supported in part by Science and Technology Fund for Research Grants of Ryukoku University, and by Grant-in-Aid for Scientific Research (No. 07640338), Ministry of Education, Science and Culture, Japan.

Abstract

The purpose of this and forthcoming papers is to obtain a better understanding of complicated bifurcations for multiple homoclinic orbits. We shall take one particular type of codimension two homoclinic orbits called orbit-flip and study bifurcations to multiple homoclinic orbits appearing in a tubular neighborhood of the original orbit-flip. The main interest of the present paper lies in the occurrence of successive homoclinic doubling bifurcations under an appropriate condition, which is a part of the entire bifurcation for multiple homoclinic orbits. Since this is a totally global bifurcation, we need an aid of numerical experiments for which we must choose a concrete set of ordinary differential equations that exhibits the desired bifurcation. In this paper we employ a family of continuous piecewise-linear vector fields for such a model equation. In order to explain the cascade of homoclinic doubling bifurcations theoretically, we also derive a two-parameter family of unimodal maps as a singular limit of the Poincaré maps along homoclinic orbits. We locate bifurcation curves for this family of unimodal maps in the two-dimensional parameter space, which basically agree with those for the piecewise-linear vector fields. In particular, we show, using a standard technique from the theory of unimodal maps, that there exists an infinite sequence of doubling bifurcations which corresponds to the sequence of homoclinic doubling bifurcations for the piecewise-linear vector fields described above. Since our unimodal map has a singularity at a boundary point of its domain of definition, the doubling bifurcation is slightly different from that for standard quadratic unimodal maps, for instance the Feigenbaum constant associated to accumulation of the doubling bifurcations is different from the standard value 4.6692....

1 Introduction

Motivation Extensive study has recently been done for bifurcations occurring in a neighborhood of a codimension two homoclinic orbit in a three-dimensional vector field, and in particular, it became known that some types of codimension two homoclinic orbits, which are bi-asymptotic to hyperbolic equilibria with real principal eigenvalues, can give rise to multiple homoclinic orbits; an N-times rounding homoclinic orbit arises under perturbation in a tubular neighborhood of the unperturbed orbit where N being an integer ([Yanagida, 1987], [Chow *et al.*, 1990], [Kisaka *et al.*, 1993a, 1993b], [Sandstede, 1993], [Homburg *et al.*, 1994]). Such a homoclinic orbit is referred to as an *N-homoclinic orbit* with

respect to the original unperturbed one. The bifurcation of such multiple homoclinic orbits are, however, still far from the complete understanding. For instance, when one varies the eigenvalues of the equilibria it has been observed, by a numerical simulation, very complicated bifurcations involving many such multiple homoclinic orbits. See, for instance, Fig. 3 and [Iori *et al.*, 1993].

The purpose of this and forthcoming papers is to obtain a better understanding of such complicated bifurcations for multiple homoclinic orbits by combining results from homoclinic bifurcation analyses with those from numerical experiments. To be more precise, we shall take one particular type of codimension two homoclinic orbits with real eigenvalues in $\mathbb{R}^3$, called *orbit-flip*, and study its bifurcation of multiple homoclinic orbits appearing in a tubular neighborhood of the original orbit-flip. The main interest of the present paper lies in the occurrence of *successive homoclinic doubling* bifurcations under an appropriate condition, which is a part of the entire bifurcations for multiple homoclinic orbits. Here the homoclinic doubling bifurcation refers to the bifurcation of a homoclinic orbit changing into a twice rounding homoclinic orbit in a tubular neighborhood of the original one. The homoclinic doubling bifurcation associated to real principal eigenvalues was first studied by Yanagida [1987] where he asserted that there are three kinds of codimension two homoclinic orbits that can undergo the homoclinic doubling bifurcations: these are now called (i) a homoclinic orbit with resonance, (ii) that of inclination-flip type, and (iii) that of orbit-flip type. See [Chow *et al.*, 1990], [Kisaka *et al.*, 1993a, 1993b] and [Sandstede, 1993] for efforts toward completing and generalizing Yanagida's original ideas concerning these three types of homoclinic doubling bifurcations. In this paper, we shall show the existence of cascade of homoclinic doubling bifurcations starting from a homoclinic orbit of orbit-flip type followed by those of inclination-flip type. Relation between such a global bifurcation and a local bifurcation from orbit-flip will also be discussed in the last section.

Continuous piecewise-linear vector fields Since the cascade of homoclinic doublings is a totally global bifurcation, we need an aid of numerical experiments for which we must choose a concrete set of ordinary differential equations that exhibits the desired bifurcation. In this paper we employ a family of *continuous piecewise-linear vector fields* for such a model equation. The advantage of using such continuous piecewise-linear (abbrev. PL) vector fields is that, firstly it is easier to analyze dynamics and bifurcations of the vector fields because of their piecewise-linearity, and secondly, according to a general theory established by the second author of this paper ([Komuro, 1988]), we can obtain a kind of normal forms for generic continuous piecewise-linear vector fields if one specifies the number of regions on which the vector field is linear, and the normal form

is completely characterized in the sense of linear conjugacy in terms of the eigenvalues at equilibria in each of these linear regions. This means that these eigenvalues are considered to be the bifurcation parameters of the normal form equations, which is suitable for our purpose of this and subsequent papers. In our case, we use the normal form of piecewise-linear vector fields with two linear regions in $\mathbb{R}^3$, and hence it possesses six parameters in total. Moreover it is easy to derive an explicit condition in terms of the eigenvalue parameters for the existence of an orbit-flip. Using this information, we can set up the model problem in a tractable way and perform very precise numerical experiments based on explicitly computed analytic formulas. The results obtained by such analyses and experiments will also be valid for general smooth vector fields, because the homoclinic bifurcation theory only uses information from the return map along the original homoclinic orbit and hence the piecewise-linearity does not lose essential information for it is constructed in the same way as in the smooth case.

Main results Using such a family of continuous piecewise-linear vector fields, we shall demonstrate the presence of the following global bifurcations in this paper: Since the original homoclinic orbit is assumed to be of orbit-flip type, it undergoes the first homoclinic doubling bifurcation and gives rise to a 2-homoclinic orbit. It then turns to be a homoclinic orbit of inclination-flip type after a slight change of parameters and thus undergoes the second doubling bifurcation creating a 4-homoclinic orbit. This 4-homoclinic orbit becomes again that of inclination-flip type for a further variation of parameters and we find 8-homoclinic orbit through the third homoclinic doubling bifurcation. By numerical experiments for our family of continuous piecewise-linear vector fields we can similarly see that each 2^k-homoclinic orbit becomes that of inclination-flip type and gives rise to a 2^{k+1}-homoclinic orbit through the homoclinic doubling bifurcation. In fact we have observed up to $2^{10} = 1024$-homoclinic orbits through these doubling bifurcations. Such precise numerical experiments could only be done by using piecewise-linear vector fields, since it is in general hard to find a homoclinic orbit as an intersection of the stable and unstable manifolds, but for piecewise-linear vector fields, those manifolds are locally given by a straight line or a plane and hence it is quite easy to find a parameter value where an orbit precisely lies on these manifolds.

In order to explain this bifurcation more theoretically, we derive a two-parameter family of unimodal maps as singular limit of the Poincaré maps along homoclinic orbits. We locate bifurcation curves for this family of unimodal maps in the two-dimensional parameter space and these curves basically agree with those for the piecewise-linear vector fields. Moreover, we can prove, using a stan-

dard technique from the theory of unimodal maps (see e.g. [Collet & Eckmann, 1980], [Milnor & Thurston, 1988], [de Melo & van Strien, 1993]), that there exists an infinite cascade of doubling bifurcations which corresponds to the sequence of homoclinic doubling bifurcations for the piecewise-linear vector fields described above. Since our unimodal map has a singularity at a boundary point of its domain of definition, the doubling bifurcation is slightly different from that for standard quadratic unimodal maps, for instance the Feigenbaum constant associated to accumulation of the doubling bifurcations is different from the standard value 4.6692.... Basic qualitative similarity between the bifurcations of our unimodal map family and the piecewise-linear vector fields strongly suggest that there does also exist a cascade of homoclinic doubling bifurcations in our family of continuous piecewise-linear vector fields in a way described by their singular limit unimodal maps.

Organization of the paper The organization of this paper is as follows. In Sec. 2, we briefly summarize basic terminology and known results for homoclinic doubling bifurcations in vector fields. In Sec. 3, we present numerical results for successive homoclinic doubling bifurcations in a family of continuous piecewise-linear vector fields, after a brief introduction to the normal form theory for such PL vector fields. In order to visualize the bifurcation phenomena and compare the results with those for vector fields, we use color diagrams where the homoclinic bifurcation sets are given as boundary curves of colored regions. We also observe more complicated bifurcation structure of homoclinic orbits in the color diagrams, but this will be treated in our forthcoming papers. In Sec. 4, we first derive a family of unimodal maps from the Poincaré maps along homoclinic orbits. The derivation works not only for the piecewise-linear vector fields but also for more general vector fields, and hence our result could be read as a general existence theorem of cascade of homoclinic doubling bifurcations from orbit-flip. We then investigate bifurcations of the unimodal map family with an aid of numerical experiments and draw the bifurcation curves by using the method of color diagrams, which shows the existence of the cascade of special period doubling bifurcations that can be interpreted as those corresponding to homoclinic doubling bifurcations in the piecewise-linear vector fields. We also compute the Feigenbaum constants for the doubling bifurcations in the unimodal maps and compare it with a similar result for the PL vector fields. Concluding remarks are given in Sec. 5 where we discuss meaning of the cascade of homoclinic doubling bifurcations and possibility of giving a mathematically rigorous proof for it.

Acknowledgement. We are grateful to T. Matsumoto, K. Iori, B. Fiedler and G. Keller for stimulating discussion and their interests to our work. We also thank A. Yamasaki for the help of computing the Feigenbaum constants.

2 Preliminaries

Consider a family of vector fields X_η on $\mathbb{R}^3$ with a hyperbolic equilibrium point O and suppose that when $\eta = 0$ it admits a homoclinic orbit Γ to the equilibrium point where the linearization matrix possesses eigenvalues $\lambda_u,\ -\lambda_{ss},\ -\lambda_s$ with $-\lambda_{ss} < -\lambda_s < 0 < \lambda_u$. The eigenvalues λ_u and $-\lambda_s$ are called principal. If X_η may possess a homoclinic orbit rounding twice in a small tubular neighborhood of the original homoclinic orbit for sufficiently small $\eta \neq 0$, such a bifurcation is referred to as *homoclinic doubling bifurcation* and the bifurcating homoclinic orbit is called a doubled homoclinic orbit or a 2-homoclinic orbit with respect to the original one, which is called the primary or 1-homoclinic orbit.

For a homoclinic orbit, we can generically expect the following two conditions to be satisfied:

(Ev) $\lambda_u \neq \lambda_s$;

(Asy) Γ is tangent at O to the eigendirection associated to $-\lambda_s$ as t tends to $+\infty$.

Besides the stable manifold $W^s(O)$, one can consider another invariant manifold which is tangent to the eigendirections associated with λ_u and $-\lambda_s$. In this paper we call it an *extended unstable manifold* and denote it by $W^{eu}(O)$. Notice that the homoclinic orbit Γ is contained in $W^{eu}(O) \cap W^s(O)$. Generically we also have

(Tr) $W^{eu}(O)$ and $W^s(O)$ intersect transversely along Γ.

A degenerate homoclinic orbit arises by breaking one of these genericity conditions, as in the following way.

Definition 2.1. Let Γ be a homoclinic orbit in the vector field $X = X_0$.

(Inc) Γ is called a *homoclinic orbit of inclination-flip type*, if (Ev) and (Asy) hold, but (Tr) does not, namely, $W^s(O)$ and $W^{eu}(O)$ are tangent along Γ;

(Orb) Γ is called a *of orbit-flip type*, if (Tr) and (Ev) hold, but (Asy) does not, namely, Γ lies in the strong stable manifold $W^{ss}(O)$;

(Res) Γ is called a *homoclinic orbit with resonance*, if (Tr) and (Asy) hold, but (Ev) does not, namely, the resonance condition $\lambda_u = \lambda_s$ is satisfied.

Remark 2.2. The proof of the center manifold theorem works as well for the existence of the extended unstable manifold $W^{eu}(O)$. See [Hirsch *et al.*, 1977] for the proof. This invariant manifold is not unique, but has the unique tangent space along the homoclinic orbit, and hence the condition (Inc), which is sometimes referred to as the strong inclination property ([Deng, 1989]), is independent of the choice of the extended unstable manifold.

Bifurcations to doubled homoclinic orbits were first studied in [Evans *et al.*, 1982] in the case of the Shil'nikov-type homoclinic orbit, along with the result of non-existence of the homoclinic doubling bifurcation for homoclinic orbits with real principal eigenvalues under the generic conditions (Asy), (Tr) and (Ev). Yanagida [1987] then claimed that there are the above three possibilities of more degenerate homoclinic orbits with real principal eigenvalues that can generate a doubled homoclinic orbit under perturbation. Since then, a lot of work has been carried out toward completing and generalizing Yanagida's original ideas.

It was shown in [Chow *et al.*, 1990] that the period-doubling bifurcation or the saddle-node bifurcation for a periodic orbit occurs in a generic two-parameter unfolding of a homoclinic orbit with resonant eigenvalues, depending whether the homoclinic orbit is twisted or non-twisted. Similar bifurcations are also shown for inclination-flip homoclinic orbits ([Kisaka *et al.*, 1993a, 1993b]) with the ratio $\nu = \frac{\lambda_s}{\lambda_u}$ of the principal eigenvalues satisfying $\frac{1}{2} < \nu < 1$. On the other hand, if the ratio ν is smaller than $\frac{1}{2}$, more complicated dynamics such as the shift dynamics accompanied by rich bifurcation phenomena in their creation possibly appear ([Deng, 1993], [Homburg *et al.*, 1994]). In particular, Homburg *et al.* [1994] proved the existence of suspension of the Smale's horseshoe in unfoldings of an inclination-flip homoclinic orbit with $\nu < \frac{1}{2},\ 2\nu < \mu = \frac{\lambda_{ss}}{\lambda_u}$ and described how N-homoclinic orbits are created or destroyed in the unfolding. Sandstede [1995] announces the existence of a shift dynamics in the unfolding of an inclination-flip homoclinic orbit with $\mu < 1,\ \mu < 2\nu$ using Lin's methods [Lin, 1990]. Recently, the existence of Hénon-like strange attractors was proven in [Naudot, 1995] using a result of Mora and Viana [1993], in the case where $1 < \mu + \nu,\ \nu < \frac{1}{2},\ \mu > K\nu$ with some large enough K. See also [Naudot, 1994] and [Kokubu & Naudot, 1995] for relevant results.

With regard to the orbit-flip, Sandstede [1993] has proven that homoclinic doubling and homoclinic N-tupling bifurcations ($N \geq 3$) as well as the shift dynamics do occur in its unfolding. There is also a numerical simulation done by Iori *et al.* [1993] for piecewise-linear vector fields involving an orbit-flip ho-

moclinic orbit which located bifurcation curves for N-homoclinic orbits with $2 \leq N \leq 11$. Our work was inspired by this last result.

Here we state a theorem concerning the homoclinic doubling bifurcations for homoclinic orbits of inclination-flip or of orbit-flip type summarizes some results from [Kisaka *et al.*, 1993b] and [Sandstede, 1993].

Theorem 2.3. *Let X_η be a generic two-parameter family of vector fields which has either an orbit-flip or an inclination-flip homoclinic orbit Γ at $\eta = 0$. Then the following holds:*

(1) If $1 < \nu = \frac{\lambda_s}{\lambda_u}$, the homoclinic doubling bifurcation does not occur.

(2) If $\frac{1}{2} < \nu < 1$ and $\mu = \frac{\lambda_{ss}}{\lambda_u} > 1$, the homoclinic doubling bifurcation occurs. More precisely, there exists a local change of parameters at $\eta = 0$

$$\varepsilon = (\varepsilon_1, \varepsilon_2) = \varepsilon(\eta),$$

and curves of the form

$$\begin{aligned} \varepsilon_2 &= \kappa_{2H}(\varepsilon_1) \quad (\varepsilon_1 \geq 0), \\ \varepsilon_2 &= \kappa_{PD}(\varepsilon_1) \quad (\varepsilon_1 \geq 0), \\ \varepsilon_2 &= \kappa_{SN}(\varepsilon_1) \quad (\varepsilon_1 \leq 0), \end{aligned}$$

in the parameter space such that a primary homoclinic orbit persists along $\varepsilon_2 = 0$ whereas a doubled homoclinic orbit bifurcates along $\varepsilon_2 = \kappa_{2H}(\varepsilon_1)$, a periodic orbit undergoes the period doubling bifurcation along $\varepsilon_2 = \kappa_{PD}(\varepsilon_1)$, and the saddle-node bifurcation occurs for periodic orbits along $\varepsilon_2 = \kappa_{SN}(\varepsilon_1)$. Moreover,

$$\begin{aligned} \kappa_{2H}(\varepsilon_1) &\approx {\varepsilon_1}^{\frac{1}{1-\nu}}, \\ \kappa_{PD}(\varepsilon_1) &\approx c{\varepsilon_1}^{\frac{1}{1-\nu}} \text{ for some } 0 < c < 1, \\ \kappa_{SN}(\varepsilon_1) &\approx c'|\varepsilon_1|^{\frac{1}{1-\nu}} \text{ for some } c' < 0. \end{aligned}$$

The bifurcation diagram is shown in Fig. 1. See also [Matsumoto *et al.*, 1993] and references therein for more information.

— Figure 1 comes here —

3 Successive Homoclinic Doublings in PL Vector Fields

3.1 Normal forms of three-dimensional two-region proper piecewise-linear vector fields

Here we shall summarize results on normal forms for three-dimensional proper two-region piecewise-linear vector fields. Since the proper condition which will be defined later is generic, they form an important class of vector fields in the study of bifurcations for continuous piecewise-linear vector fields. In particular it can be shown that normal forms of proper systems are determined by elementary symmetric polynomials of eigenvalues in each linear region as described below.

Given a non-zero vector $\alpha \in \mathbb{R}^3$, define a plane

$$V = \{x \in \mathbb{R}^3 | \langle \alpha, x \rangle = 1\}$$

(where $\langle \cdot, \cdot \rangle$ denotes the usual inner product) and half spaces

$$R_\pm = \{x \in \mathbb{R}^3 | \pm (\langle \alpha, x \rangle - 1) > 0\}.$$

Consider a vector field defined by an ordinary differential equation

$$\frac{dx}{dt} = X(x) = \begin{cases} Ax, & (x \in R_-) \\ Bx - p, & (x \in R_+), \end{cases} \tag{1}$$

where A and B are 3×3 matrices and $p \in \mathbb{R}^3$ (all elements of $\mathbb{R}^3$ are column vectors, unless otherwise stated). We call the vector field a *three-dimensional two-region piecewise-linear vector field*, and the plane V the *boundary* of the vector field. This vector field is continuous on the boundary V if and only if

$$B = A + p\alpha^T.$$

See [Matsumoto *et al.*, 1993; Lemma 2.5.1].

Definition 3.1. Two vector fields X and X' on $\mathbb{R}^3$ are *linearly conjugate* if there is a non-singular matrix $H \in GL(3, \mathbb{R})$ such that

$$HX(x) = X'(Hx) \quad \text{for all} \quad x \in \mathbb{R}^3.$$

Definition 3.2. A vector field X defined by (1) is *proper* if any A-invariant proper linear subspace $E \subset \mathbb{R}^3$ intersects with the boundary V, i.e.,

$$A(E) \subset E \quad \text{and} \quad 0 < \dim(E) < 3 \Longrightarrow E \cap V \neq \emptyset. \tag{2}$$

— **Figure 2 comes here** —

Theorem 3.3.

Any proper continuous three-dimensional two-region piecewise-linear vector field given by

$$\begin{aligned} X'(x) &= A'x + \frac{1}{2}p'\{|\langle\alpha', x\rangle - 1| + (\langle\alpha', x\rangle - 1)\} \\ &= \begin{cases} A'x, & (\langle\alpha', x\rangle - 1 \leq 0) \\ B'x - p', & (\langle\alpha', x\rangle - 1 \geq 0), \end{cases} \end{aligned}$$

is linearly conjugate to the vector field defined by

$$\begin{aligned} X(x) &= Ax + \frac{1}{2}p\{|\langle\alpha, x\rangle - 1| + (\langle\alpha, x\rangle - 1)\}, \\ &= \begin{cases} Ax, & (\langle\alpha, x\rangle - 1 \leq 0) \\ Bx - p, & (\langle\alpha, x\rangle - 1 \geq 0), \end{cases} \end{aligned}$$

where

$$\alpha = (1, 0, 0)^T, \quad p = (c_1, c_2, c_3)^T,$$

$$A = \begin{pmatrix} 0 & 1 & 0 \\ 0 & 0 & 1 \\ a_3 & a_2 & a_1 \end{pmatrix}, \quad B = \begin{pmatrix} c_1 & 1 & 0 \\ c_2 & 0 & 1 \\ c_3 + a_3 & a_2 & a_1 \end{pmatrix} = A + p\alpha^T$$

$$a_1 = \lambda_1 + \lambda_2 + \lambda_3, \;\; a_2 = -(\lambda_1\lambda_2 + \lambda_2\lambda_3 + \lambda_3\lambda_1), \;\; a_3 = \lambda_1\lambda_2\lambda_3,$$

$$b_1 = \nu_1 + \nu_2 + \nu_3, \;\; b_2 = -(\nu_1\nu_2 + \nu_2\nu_3 + \nu_3\nu_1), \;\; b_3 = \nu_1\nu_2\nu_3,$$

$$c_1 = b_1 - a_1, \;\; c_2 = b_2 - a_2 + c_1a_1, \;\; c_3 = b_3 - a_3 + a_2c_1 + a_1c_2,$$

$\lambda_1, \lambda_2, \lambda_3$ being the eigenvalues of A and ν_1, ν_2, ν_3 being those of B.

Moreover, when $\det(B) = b_3 \neq 0$, *we can write*

$$X(x) = \begin{cases} Ax, & (\langle\alpha, x\rangle - 1 \leq 0) \\ B(x - P), & (\langle\alpha, x\rangle - 1 \geq 0), \end{cases}$$

where

$$P = \left(1 - \frac{a_3}{b_3}, \frac{c_1a_3}{b_3}, \frac{c_2a_3}{b_3}\right).$$

See [Matsumoto *et al.*, 1993; Subsection 2.5.1] for the proof of this theorem.

The vector field X is determined by $\rho = (a_1, a_2, a_3, b_1, b_2, b_3) \in \mathbb{R}^6$, which will be called the *eigenvalue parameters*. Define the boundary V by

$$V = \{x \in \mathbb{R}^3 | \langle \alpha, x \rangle = 1\},$$

and set

$$V_\pm = \{x \in V | \pm \langle \alpha, Ax \rangle > 0\}.$$

If λ_i $(i = 1, 2, 3)$ is real, then the vector $\overrightarrow{OC_i}$ gives an eigenvector of A associated with λ_i, where

$$C_i = (1, \lambda_i, \lambda_i^2)^T \in V. \tag{3}$$

Assume λ_1 and λ_2 are negative real numbers and λ_3 is a positive real number, whereas ν_1 and ν_2 are a pair of complex-conjugate numbers and ν_3 is real. Since an eigenvector for λ_i is given by (3), the one-dimensional unstable eigenspace $E^u(O)$ and the two-dimensional stable eigenspace $E^s(O)$ for $O = (0, 0, 0)^T$ are given by

$$E^u(O) = \{x \in \mathbb{R}^3 | x = r(1, \lambda_3, \lambda_3^2)^T,\ \langle \alpha, x \rangle - 1 \leq 0,\ r \in \mathbb{R}\},$$

$$E^s(O) = \{x \in \mathbb{R}^3 | \langle u, x \rangle = 0,\ \langle \alpha, x \rangle - 1 \leq 0\},$$

where $u = (-1, \frac{\lambda_1 + \lambda_2}{\lambda_1 \lambda_2}, -\frac{1}{\lambda_1 \lambda_2})$. The intersection $E^s(O) \cap V$ is thus given by

$$E^s(O) \cap V = \{x = (x^1, x^2, x^3) \in \mathbb{R}^3 | \langle u, x \rangle = 0,\ x^1 = 1\}. \tag{4}$$

If $\lambda_2 < \lambda_1 < 0$, the strong stable eigenspace $E^{ss}(O)$ is given by

$$E^{ss}(O) = \{x \in \mathbb{R}^3 | x = r(1, \lambda_2, \lambda_2^2)^T,\ \langle \alpha, x \rangle - 1 \leq 0,\ r \in \mathbb{R}\}.$$

Take a point $C_3 = (1, \lambda_3, \lambda_3^2)^T \in V_+$ on the local unstable manifold of O and consider its entire orbit $\mathcal{O}(C_3)$. The integer $m > 0$ is called the *rounding number* of the orbit if

$$m = \frac{1}{2} \sharp (\mathcal{O}(C_3) \cap V).$$

Assume in particular the point C_3 lies in a homoclinic orbit of O. Then the point C_3 is called a homoclinic point *transversal* to the boundary V if there exists an integer $m > 0$, real numbers $s_1, t_i, s_i > 0$ and $x_i, y_i \in V$ $(2 \leq i \leq m)$ such that

$$y_i = e^{Bs_i}(x_i - P) + P \in V_- \quad (1 \leq i \leq m)$$

$$x_{i+1} = e^{At_{i+1}} y_i \in V_+ \quad (1 \leq i \leq m-1)$$

$$\langle \alpha, \{e^{Bs}(x_i - P) + P\} \rangle - 1 \neq 0 \quad \text{for all} \quad s \in (0, s_i) \quad (1 \leq i \leq m)$$

$$\langle \alpha, e^{At} y_i \rangle - 1 \neq 0 \quad \text{for all} \quad t \in (0, t_{i+1}) \quad (1 \leq i \leq m-1)$$
$$\langle \alpha, e^{At} y_m \rangle - 1 \neq 0 \quad \text{for all} \quad t > 0,$$

where $x_1 = C_3$. Here s_i and t_i stand for the half-return time, which is the period of time from the orbit each time leaving V until it coming back to V again.

Theorem 3.4.

Assume A and B are non-singular, and set

$$C = A^{-1}BA,$$

$$h = (1,1,1)^T, e_1 = (1,0,0)^T, e_2 = (0,1,0)^T, e_3 = (0,0,1)^T,$$

$$K(t,s) = [e_1 \alpha^T e^{-At} + e_2 \alpha^T + e_3 \alpha^T e^{Cs}]^{-1},$$

$$N = \begin{pmatrix} 0 & 1 & 0 \\ 0 & 0 & 1 \end{pmatrix}.$$

(1) If there exists $s_1 > 0$ such that

$$\langle \alpha, e^{Cs_1} C_3 \rangle - 1 = 0,$$

$$\langle u, e^{Cs_1} C_3 \rangle = 0,$$

$$\langle \alpha, e^{Cs} C_3 \rangle - 1 \neq 0 \quad \textit{for all} \quad s \in (0, s_i),$$

$$\langle \alpha, e^{At} e^{Cs_1} C_3 \rangle - 1 \neq 0 \quad \textit{for all} \quad t > 0,$$

then C_3 is a homoclinic point transversal to the boundary with the rounding number 1.

Moreover, if $\lambda_2 < \lambda_1 < 0$ and

$$e^{Cs_1} C_3 = C_2,$$

then $\mathcal{O}(C_3)$ is a homoclinic orbit of orbit-flip type. Similarly, if $\lambda_2 < \lambda_1 < 0$ and

$$\langle e_2, e^{-Bs_1}(e_2 - e_1) \rangle = 0,$$

then $\mathcal{O}(C_3)$ is a homoclinic orbit of inclination-flip type.

(2) If there exist $s_1, t_i, s_i > 0$ $(2 \leq i \leq m)$ such that

$$\langle \alpha, e^{Cs_1} C_3 \rangle - 1 = 0, \tag{5}$$

$$N(e^{At_2} e^{Cs_1} C_3 - K(t_2, s_2)h) = O, \tag{6}$$

$$N(e^{At_{i+1}} e^{Cs_i} K(t_i, s_i) - K(t_{i+1}, s_{i+1})h) = O \quad (2 \le i \le m-1), \tag{7}$$

$$\langle u, e^{Cs_m} K(t_m, s_m)h \rangle = 0, \tag{8}$$

$$\langle \alpha, e^{Cs} C_3 \rangle - 1 \neq 0 \quad \textit{for all} \quad s \in (0, s_1), \tag{9}$$

$$\langle \alpha, e^{-At} K(t_i, s_i)h \rangle - 1 \neq 0 \quad \textit{for all} \quad t \in (0, t_i) \quad (2 \le i \le m), \tag{10}$$

$$\langle \alpha, e^{Cs} K(t_i, s_i)h \rangle - 1 \neq 0 \quad \textit{for all} \quad s \in (0, s_i) \quad (2 \le i \le m), \tag{11}$$

$$\langle \alpha, e^{At} e^{Cs_m} K(t_m, s_m)h \rangle - 1 \neq 0 \quad \textit{for all} \quad t > 0, \tag{12}$$

then C_3 is a homoclinic point transversal to the boundary with the rounding number m ($m \ge 2$).

Moreover, if $\lambda_2 < \lambda_1 < 0$ and

$$e^{Cs_m} K(t_m, s_m)h = C_2,$$

then $\mathcal{O}(C_3)$ is a homoclinic orbit of orbit-flip type. Similarly, if $\lambda_2 < \lambda_1 < 0$ and

$$\langle e_2, e^{-Bs_1} e^{-At_2} e^{-Bs_2} \cdots e^{-At_m} e^{-Bs_m} (e_2 - e_1) \rangle = 0,$$

then $\mathcal{O}(C_3)$ is a homoclinic orbit of inclination-flip type.

Remark 3.5. Equations (6)-(9) are viewed as $2m$ scalar equations with $2m + 5$ variables $(\rho, s_1, t_2, s_2, \cdots, t_m, s_m) \in \mathbb{R}^{2m+5}$. Equations (10)-(12) give open conditions, and hence the solution set for (6)-(12) is 5 dimensional in $\mathbb{R}^{2m+5}$. This statement is also valid for $m = 1$. The projection of the solution set to the space $\mathbb{R}^6$ of eigenvalue parameters ρ gives a codimension one subset called the *homoclinic bifurcation set*.

3.2 Successive homoclinic doublings in piecewise-linear vector fields

— Figure 3 comes here —

We take a piecewise-linear vector field with an orbit-flip, put it into the normal form using Theorem 3.3 and regard the eigenvalues as parameters that unfold the orbit-flip homoclinic obit. Here we fix the eigenvalues $\lambda_1 = -0.2$, $\lambda_2 =$

$-0.4,\ \lambda_3 = 0.3$ at O and only vary ν_1, ν_2, ν_3. The parameter values when the orbit-flip exists are $\nu_1, \nu_2 = 0.0580073059 \pm \sqrt{-1}$ and $\nu_3 = -0.2$. In particular, for $\nu_1, \nu_2 = \sigma \pm \omega\sqrt{-1}$ and $\nu_3 = \gamma$, we mainly consider σ and γ as the bifurcation parameters in what follows, with fixed $\omega = 1.0$. Note that with this choice of eigenvalues, we have $\lambda_u = \lambda_3,\ \lambda_s = -\lambda_1,\ \lambda_{ss} = -\lambda_2$ and hence $\nu = \frac{2}{3}$.

Figure 3(a) exhibits bifurcations in the normal form family. This figure is called a color diagram, which is produced in the following way. For each choice of σ and γ while other eigenvalues being fixed, we follow the orbit starting the point C_3 in one branch of the local unstable manifold and count the rounding number m defined in the previous subsection. Each color code (except black) stands for a rounding number m, for instance, $m = 1$ (blue), 2 (yellowish green), 3 (sky blue), 4 (red), 5 (purple), 6 (yellow) and 7 (white). Higher rounding numbers m not larger than a number called $Maxcount$ are coded as $(m-1)\mathrm{mod}(7)+1$. If $m >$ Maxcount or $m = \infty$, then black is assigned. The assignment of color codes changes only when either the orbit hits the stable manifold or it becomes tangent to the boundary of the linear region, the latter case of which is not observed in our numerical experiments. In this way, it is quite easy to see the bifurcation curves for N-homoclinic orbits with various N. In Fig. 3(a), one can see, among other things, the boundary H_1 of blue region with $m = 1$ which corresponds to the 1-homoclinic bifurcation curve.

Figures 3(b) - 3(d) are successive enlargements of Fig. 3(a). In Fig. 3(b), one can observe a 2-homoclinic bifurcation curve as the boundary H_2 of yellowish green region with $m = 2$, and in Fig. 3(c), a 4-homoclinic bifurcation curve as the boundary H_4 of red region with $m = 4$. Figure 3(d) is yet another enlargement where a 8-homoclinic bifurcation curve can be observed. These homoclinic bifurcation curves are computed by using the bifurcation equation given in Theorem 3.4. Moreover, it is also possible to compute the inclination-flip bifurcation points from these bifurcation equations, and it turns out numerically that each of the branching points from k-homoclinic bifurcation curve to $2k$-homoclinic bifurcation curve corresponds to an inclination-flip homoclinic orbit, except the first one ($k = 1$). Since it is not easy to keep following such homoclinic bifurcations curves by enlargements of two-dimensional parameter space, we instead fix a line segment in the parameter space that cuts through the region where successive homoclinic doubling bifurcations are expected to occur. Enlargements of the bifurcation diagram along the line segment is much easier to carry out, and one can see in Fig. 3(e) successive homoclinic doubling bifurcations for up to $2^6 = 64$-homoclinic orbits are observed. Numerically, we have so far observed such homoclinic doubling bifurcations until giving rise to $2^{10} = 1024$-homoclinic orbits. The parameter values for these bifurcation points are give in Table 1. A 2^N-homoclinic bifurcation set for higher N is not computed, because the width

of the corresponding colored region shrinks extremely fast so that it quickly exceeds the computational limit.

— Table 1 comes here —

The parameter values for the bifurcation points given in Table 1 were computed by using UBASIC created by Y. Kida [1990], which is a variant of BASIC having the high precision real and complex arithmetic (up to 2600 digits) as well as exact rational arithmetic and arithmetic of polynomials with complex, rational, or modulo p coefficients. We have performed our numerical simulation in a way that the results of parameter values for the bifurcation points are guaranteed up to 15 digits.

Using these values, we compute the Feigenbaum constant for the homoclinic doubling bifurcations as follows. Let (γ_k, σ_k) be the value of (γ, σ) at the inclination-flip homoclinic bifurcation point for a 2^k-homoclinic orbit at which a 2^{k+1}-homoclinic orbit bifurcates. Then the Feigenbaum constant δ for the homoclinic doubling bifurcation may be computed as either

$$\delta = \lim_{k\to\infty} \frac{\gamma_k - \gamma_{k-1}}{\gamma_{k+1} - \gamma_k} \qquad \text{or} \qquad \delta = \lim_{k\to\infty} \frac{\sigma_k - \sigma_{k-1}}{\sigma_{k+1} - \sigma_k}.$$

In fact, with the values in Table 1,

$$\frac{\gamma_8 - \gamma_7}{\gamma_9 - \gamma_8} = 3.4541992606$$

and

$$\frac{\sigma_8 - \sigma_7}{\sigma_9 - \sigma_8} = 3.4539854789.$$

One can also estimate a more precise value of the Feigenbaum constant by using what is called the Aitken acceleration method, by which one can obtain the (expected) Feigenbaum constant 3.4544635128...

4 Analysis of Reduced One-Dimensional Maps

In this section we shall derive and analyze a two-parameter family of one-dimensional maps in order to study the dynamics and bifurcations that occur in an unfolding of the orbit-flip. This family is obtained by taking the singular limit of the two-dimensional return maps along the homoclinic orbit as the strong stable eigenvalue going to $-\infty$.

Let X_η be the generic two-parameter unfolding as above which possesses an orbit-flip Γ, homoclinic to a hyperbolic equilibrium point O at $\eta = 0$. Γ lies in

the intersection of the unstable and strong stable manifolds $W^u(O) \cap W^{ss}(O)$. We choose the (x, y, z)-coordinates in such a way that the local stable, unstable and strong stable manifolds are given by

$$W^u_{loc}(O) = \{x = y = 0\}, \quad W^s_{loc}(O) = \{z = 0\}, \quad W^{ss}_{loc}(O) = \{x = z = 0\}$$

in a neighborhood of O. We assume for simplicity that the vector fields X_η are uniformly smoothly linearizable in a neighborhood of O containing the unit cube $[-1, 1]^3$, and take the two cross sections

$$\Sigma^0 = \{y = 1\}, \quad \Sigma^1 = \{z = 1\}$$

which are transverse to the homoclinic orbit Γ. Then the Poincaré map for X_η along Γ will be given by composing the following two mappings:

$$\text{the local map}: \quad \Sigma^0 \to \Sigma^1 \quad ; \begin{pmatrix} x \\ 1 \\ z \end{pmatrix} \mapsto \begin{pmatrix} xz^\nu \\ z^\mu \\ 1 \end{pmatrix},$$

$$\text{the global map}: \quad \Sigma^1 \to \Sigma^0 \quad ; \begin{pmatrix} X \\ Y \\ 1 \end{pmatrix} \mapsto \begin{pmatrix} p + \alpha X + \beta Y + h.o.t. \\ 1 \\ q + \gamma X + \delta Y + h.o.t. \end{pmatrix},$$

where $\mu = \frac{\lambda_{ss}}{\lambda_u}$ and $\nu = \frac{\lambda_s}{\lambda_u}$. Note that the constants, in particular, p and q may depend on the unfolding parameter η. Since the orbit-flip exists when $(0, 0, 1)$ is mapped to $(0, 1, 0)$ under the global map, we have

$$p(\eta) = q(\eta) = 0.$$

Therefore the parameter η should be taken in such a way that

$$\left.\frac{\partial(p, q)}{\partial(\eta_1, \eta_2)}\right|_{\eta=0} \neq 0.$$

In other words, (p, q) can be thought of as unfolding parameters, and consequently, the return map h takes the form

$$\begin{pmatrix} x \\ z \end{pmatrix} \mapsto \begin{pmatrix} p \\ q \end{pmatrix} + \begin{pmatrix} \alpha & \beta \\ \gamma & \delta \end{pmatrix} \begin{pmatrix} xz^\nu \\ z^\mu \end{pmatrix} + \begin{pmatrix} h.o.t. \\ h.o.t. \end{pmatrix}.$$

Here we consider the case when the strong stable eigenvalue has a very large modulus so that we can neglect the term involving z^μ. Then the most dominant terms in the return map reduce to give a one-dimensional map

$$z \mapsto \alpha(z - q + \frac{\gamma p}{\alpha})z^\nu + q,$$

or, by rescaling the variable and parameters,

$$f(x) = (x - a - b)x^\nu + b.$$

Note that here we have assumed $\alpha > 0$ for simplicity, since the other case can be treated similarly. In what follows, we fix ν as $\frac{1}{2} < \nu < 1$ and consider the bifurcation of this two-parameter family of one-dimensional maps that are related to the dynamics of original vector fields. Recall that this range of ν corresponds to the situation described in Theorem 2.3(2). We remark that in the derivation of the one-dimensional maps, we have not used any particular form of vector fields such as piecewise-linearity, etc., and therefore the following analysis should be equally valid both for smooth vector fields and for PL vector fields.

Our goal is to show that the two-parameter family of maps

$$f(x; a, b) = (x - a - b)x^\nu + b \quad \left(\frac{1}{2} < \nu < 1\right)$$

possesses an infinite sequence of special doubling bifurcations that can be interpreted as homoclinic doubling bifurcations of corresponding vector fields. First we note that the orbit of 0 for the one-dimensional map corresponds to the unstable manifold of the equilibrium point O for the vector field, and therefore we only consider the maps on the interval $[0, f(0)] = [0, b]$ and trace the orbit of 0 as long as it stays within this interval. This map is in general a unimodal map with a minimum which can be either positive or negative depending on the parameters. In particular, the map with the parameters $(a, b) = (0, 0)$ corresponds to the vector field with an orbit-flip. The curve which can be interpreted as the persistence curve for 1-homoclinic orbit coming out from the orbit-flip point is given by the condition that 0 is a fixed point, namely $f(0) = b = 0$, whereas the bifurcation curve for 2-homoclinic orbit is given by $f^2(0) = f(b) = 0$, hence $a = b^{1-\nu}$. These two bifurcation curves nicely fit with the bifurcation diagram for the vector fields that unfold an orbit-flip.

In general homoclinic orbits for vector fields correspond to periodic orbits through 0 for these one-dimensional maps, which is given by the equation $f^N(0) = 0$. Inclination-flip homoclinic orbits are interpreted as such periodic orbits that pass through 0 and the minimum point, and hence given by the equations $f^N(0) = 0,\ f'(f^{N-1}(0)) = 0$. In particular the inclination-flip 2-homoclinic orbit is given by the equations $f^2(0) = 0$ and $f'(f(0)) = 0$, or equivalently, $(a, b) = (\nu^{\frac{1-\nu}{\nu}}, \nu^{\frac{1}{\nu}})$. Figure 4 illustrates the correspondence between bifurcation sets for vector fields and for unimodal maps. It is hard to obtain explicit analytic

expressions for the N-homoclinic bifurcation curves with $N > 2$, and hence, we use the color diagram again in order to visualize these curves.

— Figure 4 comes here —

— Figure 5 comes here —

We compute the number

$$m = \min\{n \geq 1 \mid f^n(0; a, b) \leq 0\}$$

and assign a color code for each number m. Then we can draw bifurcation sets with those assigned colors at each parameter value (a, b). Each color code (except black) stands for a rounding number m in the same way as before, namely, $m = 1$ (blue), 2 (yellowish green), 3 (sky blue), 4 (red), 5 (purple), 6 (yellow) and 7 (white) and higher rounding numbers $m \leq$ Maxcount are coded as $(m-1)\mathrm{mod}(7)+1$. If $m >$ Maxcount or $m = \infty$, black is assigned. By definition, each point of the boundary of a region with a specific color satisfies $f^m(0) = 0$ for certain number m, and hence it is interpreted as to a homoclinic bifurcation point for m-homoclinic orbit. For example, the boundary H_4 of a red region with $m = 4$ exhibits a 4-homoclinic bifurcation curve.

It can be seen that there is a curve which seems tangent to all colored regions. This curve, called the envelop, is in fact given by the condition that the minimum value of f is equal to 0, since if the minimum value is positive, then the orbit of 0 never becomes negative and hence, by the rule of color assignment, such a parameter value is colored in black. This condition of the envelop is given by $\exists x_* \in [0, b]$ such that $f'(x_*) = 0,\ f(x_*) = 0$, or equivalently,

$$a + b = \frac{1+\nu}{\nu}(\nu b)^{\frac{1}{1+\nu}}.$$

Using this expression of the envelop, we make the change of parameters from (a, b) to

$$x_* = \frac{\nu}{1+\nu}(a+b), \quad y_* = f(x_*) = b - \frac{1}{\nu}\left(\frac{\nu}{1+\nu}(a+b)\right)^{1+\nu}.$$

in such a way that the envelop is mapped to the x_*-axis. Figure 5(b) exhibits the color diagram with these new parameters, where we can more easily see the bifurcations, in particular several successive homoclinic doubling bifurcations. This situation can be seen in more detail by taking $(\log x_*, \log y_*)$ as new parameters. See Fig. 5(c). Observe that the homoclinic doubling bifurcations successively occur from 2-homoclinic orbit to $2^{10} = 1024$-homoclinic orbit.

Since the homoclinic doubling bifurcation in vector fields corresponds to 0 being a periodic point that passes through the minimum of the unimodal map f, we shall rigorously show that there exists an infinite sequence of such successive doubling bifurcations in the family of unimodal maps.

Theorem 4.1. *The two-parameter family of one-dimensional unimodal maps $f_{a,b}$ has a cascade of doubling bifurcations that can be interpreted as cascade of homoclinic doublings in the above sense.*

Proof. We have only to consider the case where the minimum value of the unimodal map is 0. This will reduce the two-parameter family of unimodal maps to that with only one parameter:

$$\tilde{f}_b = \left\{ x - \frac{1+\nu}{\nu} (\nu b)^{\frac{1}{1+\nu}} \right\} x^\nu + b,$$

since the condition that the minimum is equal to 0 is given by

$$y_* = b - \frac{1}{\nu} \left(\frac{\nu}{1+\nu} (a+b) \right)^{1+\nu} = 0.$$

The family $\tilde{f}_b$ is a C^1-family of unimodal maps that are continuous and onto over the interval $[0, b]$, and are of C^1 on $(0, b]$. Therefore this is almost what is called the full family in the sense of Collet-Eckmann, for which the intermediate value theorem for kneading sequences holds. See [Collet & Eckmann, 1980], in particular Theorem III.1.1 for the detail. We can apply this theorem to our family by modifying the proof of Theorem III.1.1 in [Collet & Eckmann, 1980], or more simply by looking at the second iterate $\tilde{f}_b^2$ as follows: Since we assume the exponent ν satisfying $\frac{1}{2} < \nu < 1$, it is easy to see that $\tilde{f}_b^2$ restricted to $[x_0, b]$ is exactly a full family of C^1-unimodal maps without any singularity, where x_0 stands for the unique fixed point for $\tilde{f}_b$. Since we have computed the existence of the first doubling bifurcation point analytically, we conclude that the cascade of doubling bifurcations occurring in $\tilde{f}_b^2$ gives the desired sequence.

— Table 2 comes here —

— Figure 6 comes here —

We have numerically computed, again by using UBASIC [Kida, 1990], the Feigenbaum constants for the doubling bifurcations in the family $\tilde{f}_b$ with various exponents ν. See Fig. 6. It should be noted that when $\nu = 1$, the map becomes quadratic and hence the Feigenbaum constant must be equal to the

standard value 4.6692..., but it is not the case when $\frac{1}{2} < \nu < 1$. Our data for the Feigenbaum constants resemble to similar data for the unimodal maps $x \mapsto 1 - a|x|^\zeta$ with $1 < \zeta < 12$ computed in [Hu & Satija, 1983] where the exponent ζ corresponds to 2ν in our case. From our computation, we get the Feigenbaum constant for $\nu = \frac{2}{3}$ is 3.4544613..., which is quite close to the corresponding value 3.4544635128... given in Sec. 3 for the homoclinic doubling bifurcations in the vector fields.

5 Concluding remarks

In this paper, we have shown the existence of cascade of homoclinic doubling bifurcations from a vector field with a homoclinic orbit of orbit-flip type. We have verified it by performing numerical simulation for piecewise-linear vector fields, which is a convenient object for accurate numerical computation because of its piecewise-linearity. This result is confirmed by deriving a family of one-dimensional unimodal maps that seems to reflect essential features of bifurcations in the vector fields when the strong stable eigenvalue has a large modulus. We have given a rigorous mathematical proof for the existence of an infinite sequence for successive doubling bifurcations in the one-dimensional maps that are interpreted as homoclinic doublings in the corresponding vector fields. The bifurcation aspects in both vector fields and unimodal maps are viewed via color diagrams. By comparing these color diagrams as well as the corresponding Feigenbaum constants, we believe that there exists such a cascade of homoclinic doublings in vector fields as well, which will give a new bifurcation scenario to chaotic dynamics.

Importance of studying the accumulation of homoclinic doublings is that it can provide new information about the boundary of chaotic dynamics in the parameter space. It has been known as in Theorem 2.3 that a homoclinic doubling bifurcation accompanies a period doubling bifurcation for periodic orbits that bifurcate from the homoclinic orbits ([Chow *et al.*, 1990], [Kisaka *et al.*, 1993a, 1993b], [Sandstede, 1993]). See also Figs. 7 and 8 for the locus of the first few bifurcation curves from 1-homoclinic orbits. Similar bifurcation structure repeatedly appear for higher homoclinic orbits, and the period doubling bifurcation curves seem converging to a certain curve in the parameter space. Furthermore the Feigenbaum constant for the period doubling bifurcations along a line transverse to the period doubling bifurcation curves gives the standard value 4.6692... according to our numerical simulation both for the PL vector fields and to the reduced one-dimensional maps.

— Figure 7 comes here —

— Figure 8 comes here —

The accumulation of period doubling bifurcations give one of the most typical routes to chaos which is a codimension one phenomenon, namely, one can observe it in a one-parameter family. On the other hand, a homoclinic orbit is considered to be related with the sudden disappearance of chaotic attractor as known by the name "crisis". The accumulation of homoclinic doublings thus corresponds to a corner point in the parameter space where the fate of chaotic attractors drastically change.

In this respect, it is quite interesting to notice that the Feigenbaum constant for the homoclinic doubling bifurcations is different from that for the usual period doublings; the latter gives the standard value 4.6692..., whereas the former depends on the eigenvalues at an equilibrium point to which the homoclinic orbits are asymptotic, and the value is in general different from the standard one. This may provide a hint for a better understanding of chaotic dynamics in vector fields rather than unimodal maps or diffeomorphisms, because the homoclinic doubling bifurcation is a unique bifurcation phenomenon in vector fields.

Another interesting feature of the bifurcations studied in this paper is a difference between two kinds of codimension two homoclinic orbits, namely, the orbit-flip and the inclination-flip. Our numerical results show that an orbit-flip gives rise to successive homoclinic doublings through inclination-flips, but not vise versa, namely, none of the inclination-flip homoclinic orbits does not seem to create another orbit-flip. This may be due to the specific form of normal form equations, but could be the case in a more general situation. Note that bifurcations from orbit-flip and inclination-flip homoclinic orbits are fairly similar, because both of them act as changing twisting nature of nearby trajectories around the homoclinic orbit. This similarity has been partly explained by Nii [1995] from a topological point of view, and will further be investigated in our forthcoming papers.

We shall now briefly discuss about the possibility of giving a rigorous mathematical proof for the existence of the cascade of homoclinic doubling bifurcations. Needless to say, the main difficulty lies in the fact that this bifurcation is totally of global nature and hence one needs to trace infinitely many doubling bifurcations all the way in the parameter space, which is of course a very hard task in general. For one-dimensional maps, we can make use of the kneading theory which enables us to keep track of bifurcations in a combinatorial way. Therefore, one way of showing the existence of the cascade in vector fields may be to relate the bifurcations in one-dimensional maps with the vector field counterparts in a more rigorous manner. This will be a type of singular pertur-

bation argument from a one-dimensional map in singular limit to a perturbed two-dimensional return map.

A similar but slightly easier problem has been studied in [Kokubu & Naudot, 1995] where it is shown that there exist infinitely many inclination-flip homoclinic orbits in an unfolding of a codimension three homoclinic orbit which is called an inclination-flip homoclinic orbit of weak type. The motivation again lies in tracing global bifurcations involving infinitely many codimension two homoclinic orbits such as inclination-flips, and the main idea in [Kokubu & Naudot, 1995] was to reduce such a global bifurcation problem into a local problem by focusing on a more degenerate situation where the global bifurcations shrink down to local bifurcations occurring in an unfolding of the degenerate homoclinic orbit. This kind of ideas may also be useful for our problem in this paper and will also be exploited furthermore in the subsequent papers.

In this paper, we have mainly focused upon successive homoclinic doubling bifurcations, but as we see in the figures in Sec. 4, we can find various kind of other homoclinic bifurcations. We have also observed more complicated bifurcations when we go to the situation where the ratio of eigenvalues $\nu = \frac{\lambda_s}{\lambda_u}$ becomes smaller than $\frac{1}{2}$ or $\mu = \frac{\lambda_{ss}}{\lambda_u}$ smaller than 1. It will be an interesting problem to study how the situation changes from the case where we only have a homoclinic doubling bifurcation ([Kisaka *et al.*, 1993a, 1993b], [Sandstede, 1993]) to the case where there exists a chaotic dynamics and accompanying complicated bifurcations that lead to chaos ([Homburg *et al.*, 1994], [Sandstede, 1993], [Naudot, 1995]). We also leave this problem for our future publications.

References

[1990] S.-N. Chow, B. Deng and B. Fiedler, Homoclinic bifurcation at resonant eigenvalues, *J. Dynam. Diff. Eq.* **2** (1990) 177–244.

[1980] P. Collet and J.-P. Eckmann, *Iterated Maps of the Interval as Dynamical Systems*, 1980, Birkhäuser.

[1989] B. Deng, The Sil'nikov problem, exponential expansion, strong λ-lemma, C^1-linearization, and homoclinic bifurcation, *J. Diff. Eq.* **79** (1989) 189–231.

[1993] B. Deng, Homoclinic twisting bifurcations and cusp horseshoe maps, *J. Dynam. Diff. Eq.* (1993) 417–467.

[1982] J. W. Evans, N. Fenichel and J. A. Feroe, Double impulse solutions in nerve axon equations, *SIAM J. Appl. Math.* **42** (1982) 219–234.

[1978] M. Feigenbaum, Quantitative universality for a class of nonlinear transformations, *J. Stat. Phys.* **19** (1978) 25–52; *ibid.* **21** (1979) 669–709.

[1994] A. J. Homburg, H. Kokubu and M. Krupa, The cusp horse-shoe and its bifurcations in the unfolding of an inclination-flip homoclinic orbit, *Ergod. Th. Dynam. Sys.* **14** (1994) 667–693.

[1977] M. Hirsch, C. Pugh and M. Shub, *Invariant Manifolds*, Lect. Notes in Math., Vol. 583, 1977, Springer.

[1983] B. Hu and I. I. Satija, A spectrum of universality classes in period doubling and period tripling, *Phys. Lett. A.* **98** (1983) 143–146.

[1993] K. Iori, E. Yanagida, and T. Matsumoto, N-homoclinic bifurcations of piecewise-linear vector fields, in *Structure and Bifurcations of Dynamical Systems* (Ed. S. Ushiki), Advanced Series in Dynamical Systems, Vol. 11, 1993, pp. 82–97, World Scientific.

[1990] Y. Kida, UBASIC86, Ver. 8.1 User's Manual (in Japanese), 1990, Nihon Hyouronsya.

[1993a] M. Kisaka, H. Kokubu and H. Oka, Supplement to homoclinic doubling bifurcation in vector fields, in *Dynamical Systems* (Eds. R. Bamon *et al.*), Pitman Research Notes in Math., Vol. 285, 1993, pp. 92–116, Longman Scientific & Technical.

[1993b] M. Kisaka, H. Kokubu and H. Oka, Bifurcations to N-homoclinic orbits and N-periodic orbits in vector fields, *J. Dynam. Diff. Eq.* **5** (1993) 305–357.

[1995] H. Kokubu and V. Naudot, Existence of infinitely many homoclinic doubling bifurcations from some codimension three homoclinic orbits, Preṕublication de Univ. Bourgogne, n^o 95-61, 1995.

[1988] M. Komuro, Normal forms of continuous piecewise-linear vector fields and chaotic attractors, Part I, *Japan J. Appl. Math.* **5** (1988) 257–304; Part II, *ibid.* **5** (1988) 503–549.

[1992] M. Komuro, Bifurcation equations of continuous piecewise-linear vector fields, *Japan J. Ind. Appl. Math.* **9** (1992) 269–312.

[1990] X.-B. Lin, Using Melnikov's method to solve Silnikov problems, *Proc. Royal Soc. Edinburgh* **116A** (1990) 295–325.

[1993] T. Matsumoto, M. Komuro, H. Kokubu, and R. Tokunaga, *Bifurcations – Sights, Sounds, and Mathematics*, 1993, Springer.

[1993] W. de Melo and S. van Strien, *One-Dimensional Dynamics*, 1993, Springer.

[1988] J. Milnor and W. Thurston, On iterated maps of the interval, in *Dynamical Systems*, Lect. Notes Math., Vol. 1342, 1988, pp. 465–563, Springer; the original preprint, 1977, Princeton.

[1993] L. Mora and M. Viana, Abundance of strange attractors, *Acta Math.* **171** (1993) 1–71.

[1994] V. Naudot, Hyperbolic dynamics in the unfolding of a degenerate homoclinic orbit, preprint, 1994.

[1995] V. Naudot, Strange attractor in the unfolding of an inclination-flip homoclinic orbit, to appear in *Ergod. Th. Dynam. Sys.*

[1995] S. Nii, N-homoclinic bifurcations for homoclinic orbits changing its twisting, to appear in *J. Dynam. Diff. Eq.*

[1990] M. R. Rychlik, Lorenz-attractors through Šil'nikov-type bifurcation, Part I, *Ergod. Th. Dynam. Sys.* **10** (1990) 793–821.

[1993] B. Sandstede, Verzweigungstheorie homokliner Verdopplungen, Ph. D. thesis, University of Stuttgart, 1993.

[1995] B. Sandstede, in preparation.

[1987] E. Yanagida, Branching of double pulse solutions from single pulse solutions in nerve axon equations, *J. Diff. Eq.* **66** (1987) 243–262.

Captions

Table 1 The values of (γ, σ) at the k-th inclination-flip homoclinic bifurcation points (IF_k) for $k = 2, 3, ..., 9$, from which a 2^{k+1}-homoclinic orbit bifurcates.

Table 2 Successive homoclinic doublings and the Feigenbaum constant. For each value of ν, the parameter values x_* for inclination-flip 2^k-homoclinic orbits ($k = 1, 2, ...10$) are shown, together with approximate values of the corresponding Feigenbaum constant δ computed from those data.

Figure 1 Homoclinic doubling bifurcation diagram.

Figure 2 Continuous piecewise-linear vector field and a homoclinic orbit.

Figure 3 Color-coded homoclinic bifurcation diagram for three-dimensional continuous piecewise-linear vector field with $\lambda_1 = -0.2, \lambda_2 = -0.4, \lambda_3 = 0.3, \omega = 1.0$. (a) Horizontal axis: $0.0 \geq \gamma \geq -0.26$, Vertical axis: $0.0 \leq \sigma \leq 0.3$, Maxcount = 20. (b) Enlargement of (a). Horizontal axis: $0.0 \geq \gamma \geq -0.26$, Vertical axis: $0.1 \geq H_1(\gamma) - \sigma \geq 0.0$, where $\sigma = H_1(\gamma)$ is a function which gives the 1-homoclinic bifurcation curve H_1 in (a). Maxcount = 20. (c) Enlargement of (b). Horizontal axis: $0.0 \geq \gamma \geq -0.16$, Vertical axis: $0.01 \geq H_2(\gamma) - \sigma \geq 0.0$, where $\sigma = H_2(\gamma)$ is a function which gives the 2-homoclinic bifurcation curve H_2 in (b). Maxcount = 20. (d) Enlargement of (c). Horizontal axis: $0.0 \geq \gamma \geq -0.08$, Vertical axis: $0.001 \geq H_4(\gamma) - \sigma \geq 0.0$, where $\sigma = H_4(\gamma)$ is a function which gives the 4-homoclinic bifurcation curve H_4 in (c). Maxcount = 20. (e) Successive enlargements of a line segment in (d) with $\gamma = -0.074$ fixed, Maxcount = 128. Left: $0.1537311 \leq \sigma \leq 0.1537811$, that corresponds to $0.00010 \geq H_4(\gamma) - \sigma \geq 0.00015$. Middle: $0.1537433 \leq \sigma \leq 0.1537437$. Right:$0.1537433998075 \leq \sigma \leq 0.1537433998125$.

Figure 4 Correspondence between bifurcation sets for vector fields and those for their reduced one-dimensional unimodal maps. The shaded region exhibits the set of parameter values whose color code is 3.

Figure 5 Color-coded bifurcation diagram for the one-dimensional map $f(x) = (x - a - b)x^{\nu} + b$ where $\nu = 0.8$. (a) (a, b)-parameter space: $0.0 \leq a \leq 2.0$, $0.0 \leq b \leq 5.0$, Maxcount $= 30$. (b) (y_*, x_*)-parameter space: $0.0 \geq y_* \geq -0.1$, $0.0 \leq x_* \leq 2.0$, Maxcount $= 30$. (c) Successive homoclinic doubling bifurcations. Horizontal axis: $-9.5 \leq \log_{10} y_* \leq 0.0$, Vertical axis: $\log_{10} b_0 \geq \log_{10}(b_0 - x_*) \geq -8.0$, where $b_0 = 1.151739$ and $\log_{10} b_0 = 0.061354$, Maxcount $= 1024$.

Figure 6 The graph of (approximate) Feigenbaum constants as a function of ν.

Figure 7 (Above) Bifurcation curves in the (σ, γ)-space for the PL vector fields; the homoclinic bifurcation curves for 1-homoclinic orbits (1-Hom) and 2-homoclinic orbits (2-Hom), the period doubling bifurcation curve (1-PD) are drawn. (Below) Its enlargement in the parallelogram with the vertices $(\sigma_1, \gamma_1) = (0.2, -0.07)$, $(0.13, -0.07)$, $(0.07, -0.22)$, $(0.0, -0.22)$.

Figure 8 (Above) Similar bifurcation curves in (x_*, y_*)-space for the reduced one-dimensional maps; the homoclinic bifurcation curves for 1-homoclinic orbits (1-Hom) and 2-homoclinic orbits (2-Hom), the period doubling bifurcation curves for 1-periodic orbits (1-PD) and 2-periodic orbits (2-PD), and the saddle-node bifurcation curve for 2-periodic orbits (2-SN) are drawn. (Below) Its enlargement.

	γ	σ
IF_2	-0.11436844171844715940399 19	0.12459678557099274364578 72
IF_3	-0.08930762967288370613181 33	0.14252342878142614938869 95
IF_4	-0.08191761929594808951169 69	0.14788866833206685817705 55
IF_5	-0.07975781088670084720642 97	0.14946846611475387467769 17
IF_6	-0.07913066931685758176791 45	0.14992831065234162856724 50
IF_7	-0.07894896039594972625922 44	0.15006164394153160343189 65
IF_8	-0.07889634538737446503949 22	0.15010025970200751111697 66
IF_9	-0.07888111320051836410827 90	0.15011143976072861169662 35

Table 1:

	$\nu = 0.501$	$\nu = 0.60$	$\nu = 0.70$	$\nu = 0.80$	$\nu = 0.90$	$\nu = 1.00$
$k = 1$	0.251694	0.426827	0.600774	0.756593	0.889525	0.999999
$k = 2$	0.287954	0.593588	0.847700	1.047174	1.198263	1.310702
$k = 3$	0.289910	0.646458	0.920318	1.125175	1.274332	1.381547
$k = 4$	0.290711	0.663550	0.940856	1.145058	1.292127	1.396945
$k = 5$	0.291060	0.669037	0.946594	1.150062	1.296239	1.400253
$k = 6$	0.291214	0.670792	0.948191	1.151317	1.297187	1.400961
$k = 7$	0.291281	0.671353	0.948635	1.151632	1.297405	1.401113
$k = 8$	0.291311	0.671532	0.948758	1.151711	1.297455	1.401146
$k = 9$	0.291325	0.671590	0.948792	1.151730	1.297467	1.401153
$k = 10$	0.291330	0.671608	0.948802	1.151735	1.297469	1.401154
δ	2.259316	3.131465	3.598464	3.990066	4.342408	4.669195

Table 2:

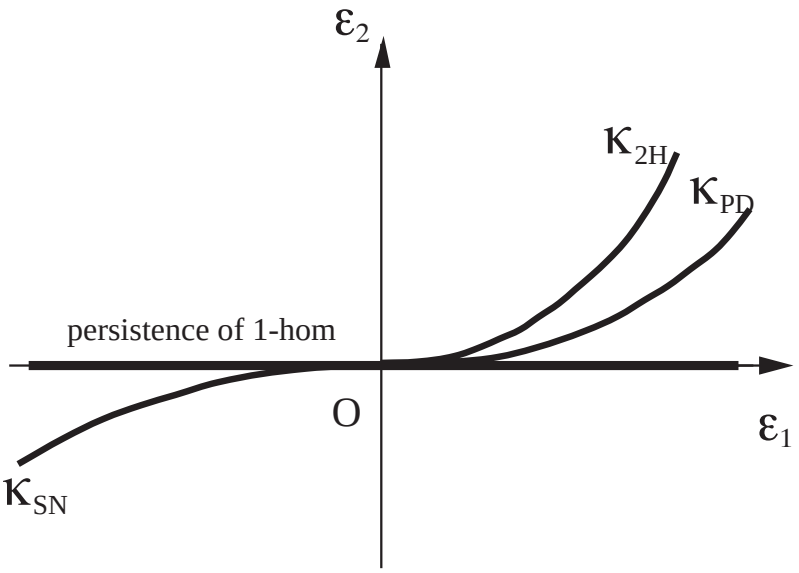

Figure 1:

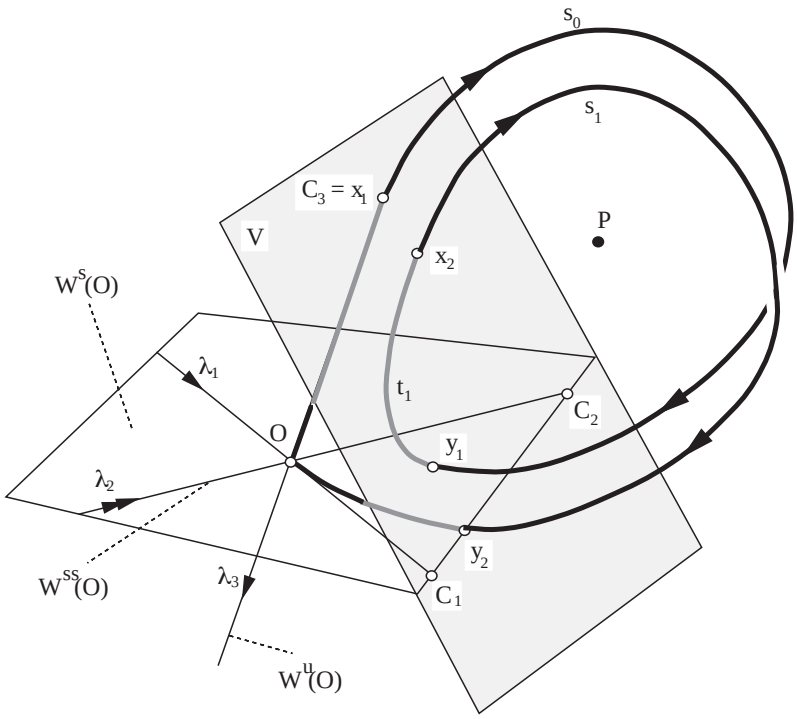

Figure 2:

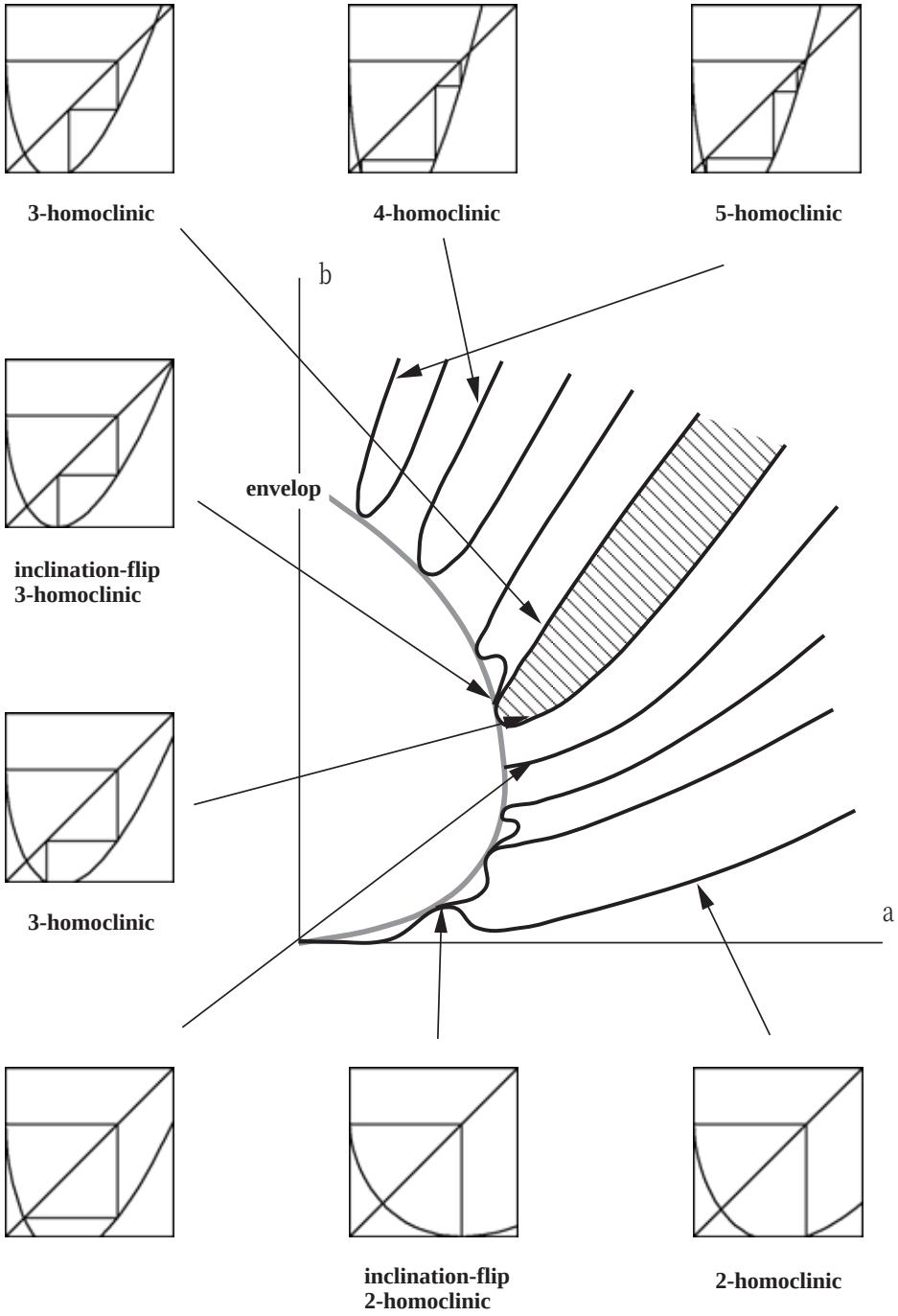
3-homoclinic
4-homoclinic
5-homoclinic
b
envelop
inclination-flip
3-homoclinic
3-homoclinic
a
inclination-flip
2-homoclinic
2-homoclinic

Figure 4:

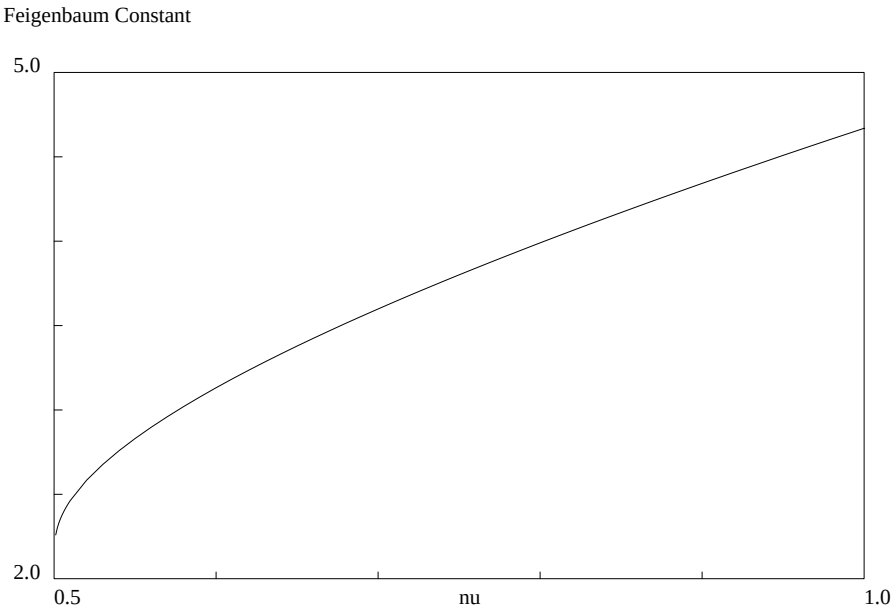

Figure 6:

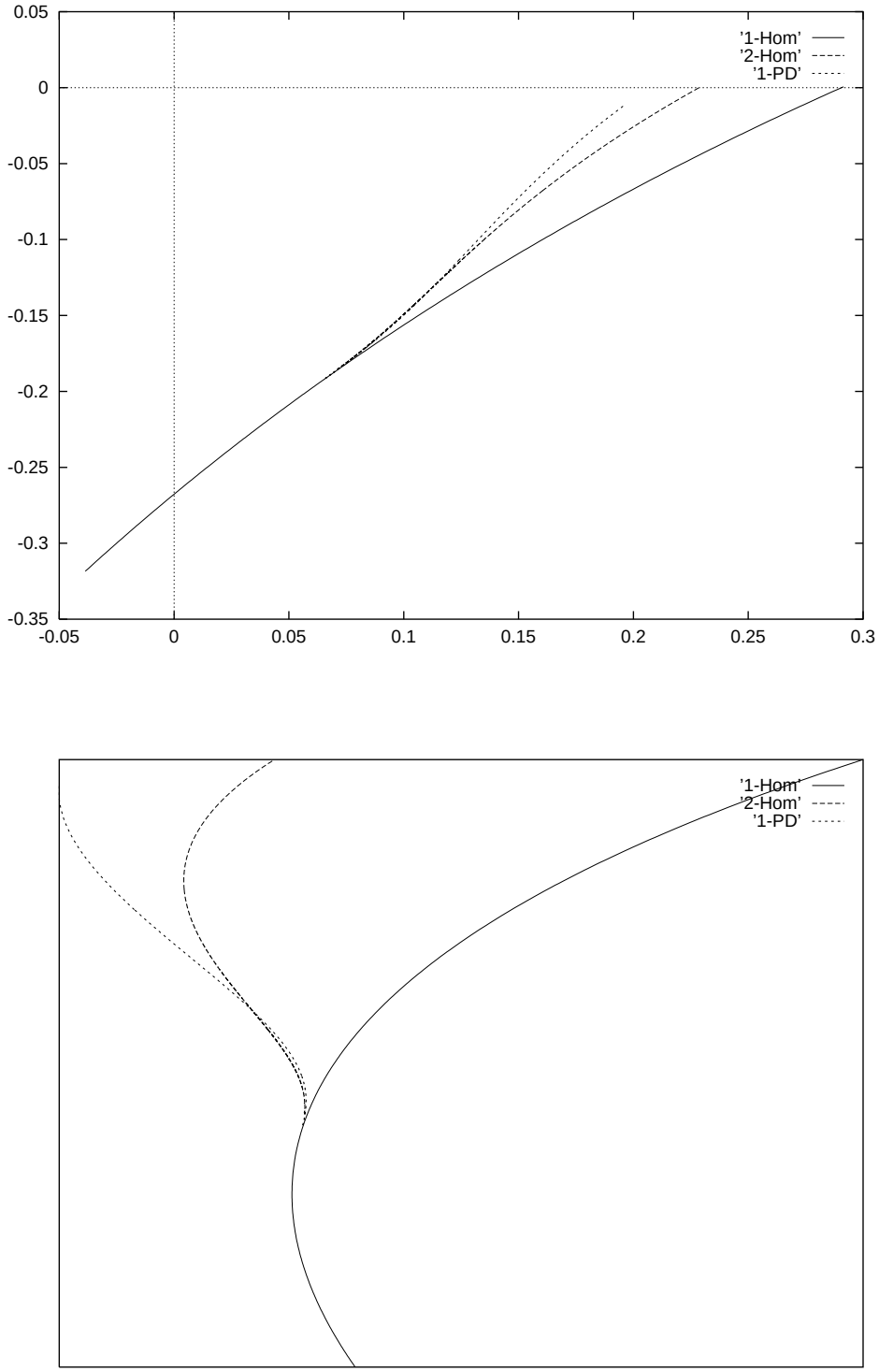
'1-Hom'
'2-Hom'
'1-PD'
0.05
0
-0.05
-0.1
-0.15
-0.2
-0.25
-0.3
-0.35
-0.05
0
0.05
0.1
0.15
0.2
0.25
0.3
'1-Hom'
'2-Hom'
'1-PD'

Figure 7:

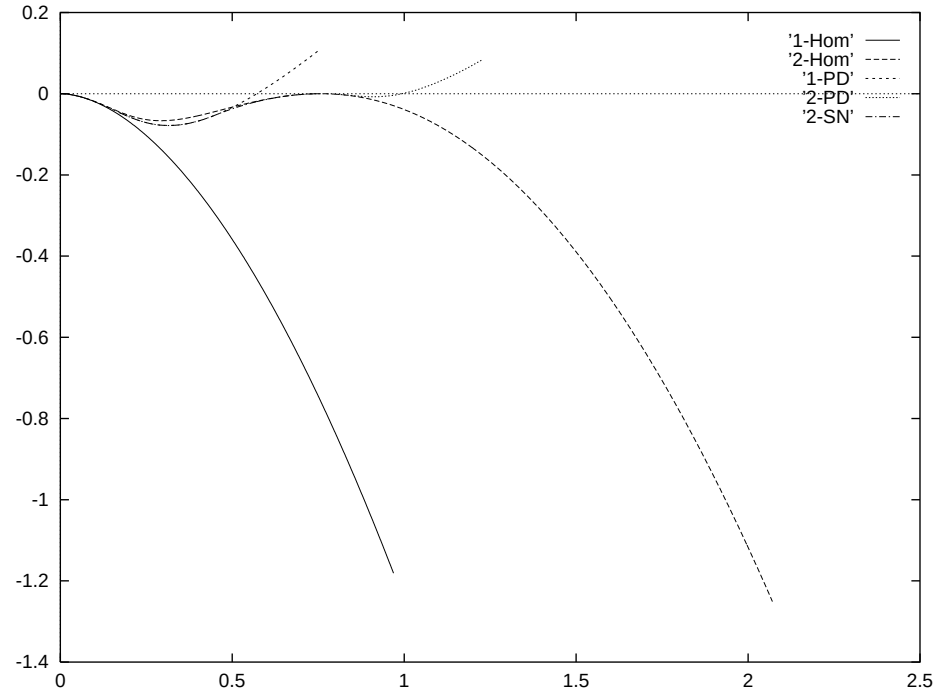
'1-Hom'
'2-Hom'
'1-PD'
'2-PD'
'2-SN'
0.2
0
-0.2
-0.4
-0.6
-0.8
-1
-1.2
-1.4
0
0.5
1
1.5
2
2.5

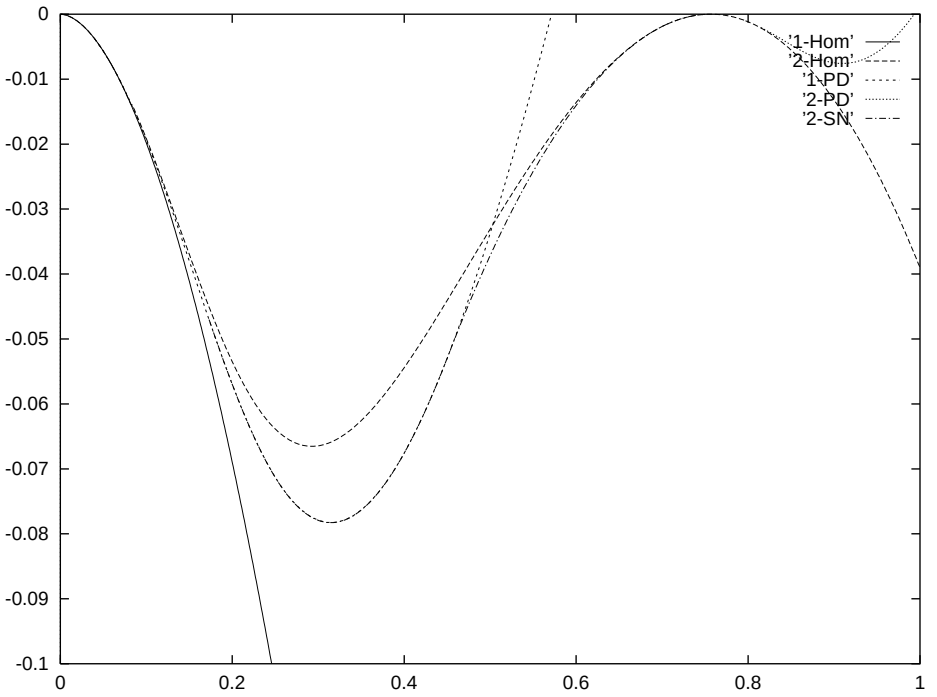
'1-Hom'
'2-Hom'
'1-PD'
'2-PD'
'2-SN'
0
-0.01
-0.02
-0.03
-0.04
-0.05
-0.06
-0.07
-0.08
-0.09
-0.1
0
0.2
0.4
0.6
0.8
1

Figure 8: